JOURNAL OF CATALYSIS 125, 311–324 (1990)

Coke and Deactivation

II. Formation of Coke and Minor Products in the Catalytic Cracking of *n*-Hexene on USHY Zeolite

W. A. GROTEN, B. W. WOJCIECHOWSKI,* AND B. K. HUNTER†

*Department of Chemical Engineering and †Department of Chemistry, Queen's University, Kingston, Ontario, Canada K7L 3N6

Received May 31, 1989; revised March 2, 1990

The minor products formed during the conversion of *n*-hexene on USHY zeolite were examined. GC-MS analyses of the concentrated products show the presence of alkylated monocyclic and polycyclic olefins, alkylated mononuclear and polynuclear aromatics up to and including C_{18} species, and acyclic paraffins and olefins up to C_{21}. Relative to the corresponding cycloolefins, only trace amounts of acyclic diolefins were detected, suggesting that dehydrogenation of the surface species is normally preceded by a cyclization reaction. The spectrum of species detected presents a cohesive picture of their development from the linear feed (*n*-hexene) to mono- and polycyclic species and finally to mono- and polynuclear aromatics. The presence of acyclic C_{21} species indicates that tetramers of the feed are formed, although the tetramers themselves were not detected. The largest linear molecule detected was pentadecane. ^{13}C CP/MAS-NMR of the coked catalyst indicates that the irreversibly adsorbed surface species consist of aromatic and aliphatic structures. Some highly deshielded structures with chemical shifts up to 150 ppm have been observed as well as structures in the −2-ppm range. Spectra taken at various times on stream indicate that the structure of the irreversibly adsorbed "coke" reaches a steady state within the first 20 s of reaction and does not change subsequently. The loading of carbon in the coke per gram of catalyst follows a similar pattern: a rapid increase in the first 20 s of reaction followed by very little subsequent growth with increasing time on stream. The ^{29}Si MAS-NMR spectra indicate a variation in the Si(1Al) adsorption peak linewidth with time on stream. The pattern of broadening observed suggests that coke is formed in localized regions and distributes itself over the rest of the catalyst surface on a time scale of minutes. This long period of redistribution, coupled with the rapid decay of the catalyst in this system, suggests that both coking and reactant conversion occur mainly near the surface of the zeolite crystallites. After the catalyst is essentially deactivated the coke continues to migrate over the catalyst surface.

INTRODUCTION

In a previous paper (*1*) the stoichiometry of coke formation from *n*-hexene on USHY at 305°C was outlined. The initial coke was found to consist of olefinic species (C_nH_{2n}) and dehydrogenated species with the stoichiometry C_nH_{2n-2}. Its average carbon chain length and molecular weight were determined to be 5.1 and 70.4, respectively. Dehydrogenation to the polynuclear aromatic form of coke, which is often discussed in the literature (*2, 3*), must occur by subsequent reactions of these surface species with gas-phase olefins. Our observation of measureable amounts of alkylated cycloolefins as both primary and secondary products of the reaction suggests that the first step in the dehydrogenation of the surface species is a cyclization reaction.

In this our second paper on coke and *n*-hexene reactions, coke formed during these reactions is directly examined using ^{13}C CP/MAS-NMR and elemental analysis, while its interactions with the catalyst are examined using ^{29}Si MAS-NMR. We will also deal with the mechanisms of formation of the minor cyclic products observed in our stud-

0021-9517/90 $3.00

ies. It is our contention that these minor products are related to the formation of the aromatic portion of coke as precursors or as byproducts of the coking reaction.

EXPERIMENTAL

1-Hexene of 96.357% purity, obtained from Aldrich, was used without further purification. The major impurities were skeletal isomers of *n*-hexene, as well as *n*-hexane and 1-octene. A detailed analysis of the feed has been presented previously (*1*).

The catalyst, ultrastable HY (USHY), was prepared from NaY (BDH Chem., Lot No. 45912, 13Y SK40) by repeated exchange of the catalyst with ammonium nitrate solution. Between exchanges the catalyst was dried at 110°C for 24 h, then calcined at 500°C for 2 h. After the last exchange the catalyst was steamed for 24 h at 200°C. The degree of exchange of the USHY was 99.7%. The bulk Si/Al ratio was determined by neutron activation analysis to be 3.30 while the framework ratio, Si/Al_{FW}, was found to be 12.00 by ^{29}Si MAS-NMR. Although determination of the framework Si/Al ratio of USHY catalysts by NMR may not yield exact results (*4*) due to the over lap of the $Si(OSi)_3(OAl)_1$ peak with the $Si(OSi)_3(OH)_1$ peak, our ^{29}Si spectra showed no evidence of the $Si(OSi)_3(OH)_1$ peak when cross-polarization was used. We therefore believe the framework ratio determined by NMR to be accurate.

Each experimental run was carried out in an isothermal plug flow reactor. Integral conversion was obtained by collecting the products and unconverted reactant at the exit to the reactor and measuring the amount of reactant converted. Conversion was defined as all products other than 1-, 2-, or 3-hexene isomers. Reactions were carried out at 305 and 500°C at 101.3 kPa. Time on stream was varied from 1.5 min to 20 min for a series of catalyst-to-reactant ratios. Table 1 lists the results of the experimental runs conducted. The detailed experimental procedures and apparatus are outlined elsewhere (*1, 5*). The minor product analysis

TABLE 1

Experimental Conditions and Average Conversions

Temp (°C)	Time on stream (s)	Catalyst-to-reactant (wt)	Conversion (%)
305	110	0.0094	0.99
	129		0.75
	193		0.85
	259		0.84
	399		0.53
	709		0.76
	1234		0.52
	99	0.024	2.00
	113		2.44
	129		2.69
	154		2.89
	258		2.64
	706		2.74
	1138		3.20
	1156		3.09
	111	0.0491	6.58
	154		6.81
	193		8.89
	399		7.52
	875		9.39
	1141		12.45
	1167		11.15
500	104	0.0125	11.05
	124		12.44
	165		12.89
	458		18.38
	754		21.88
	1097		18.78
	105	0.0187	13.42
	124		13.26
	165		15.53
	457		17.17
	761		27.87
	761		27.78
	1157		25.20
	104	0.0797	60.34
	178		59.72
	144		64.30
	164		64.95
	274		72.92
	455		78.29
	749		83.68
	1121		82.96

was carried out by taking the products which are liquid at room temperature and concentrating them by vacuum distillation at 3.9 kPa and 25°C to approximately 1% of their original volume. The resulting concentrate from this process was examined using a Finnigan automated GC-MS with a 60-m, SE54, capillary column. Products were eluted at 30°C for 10 min followed by a temperature-programmed ramp of 5°C/min to 300°C.

In experimental runs in which MAS-NMR analysis was applied, the reactor was packed with catalyst pellets (mesh size 80–100) and inert silica (SiO_2) (mesh size 40–60). The standard experimental procedure (*5*) was then followed up to the point of regeneration. At this point the reactor was allowed to cool to room temperature under a nitrogen atmosphere. The reactor was sealed, then taken to a glovebox where, again under nitrogen, the catalyst was separated from the inert silica by sieving. Next the coked catalyst was finely ground and packed in an air-tight spinner. This procedure precluded any effect atmospheric moisture and oxygen may have on the NMR spectra. The catalytically inert silica exhibits a single sharp (half-height width = 0.4 ppm) peak at −128 ppm; thus, even if the separation process had left trace amounts of silica in the coked catalyst, the NMR lines of the zeolite would not be affected.

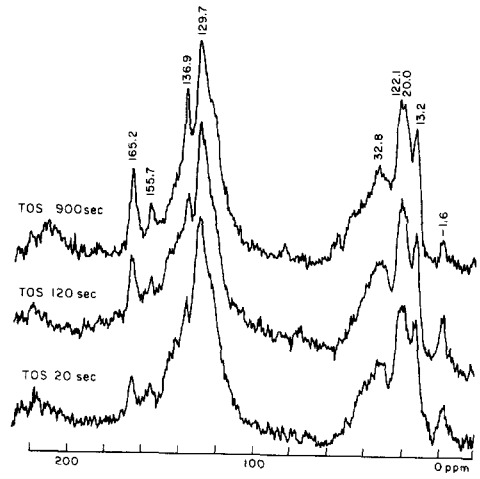

FIG. 1. ^{13}C CP/MAS-NMR spectra of coke. Reaction conditions: 305°C; catalyst/reactant ratio: 0.0491. NMR experimental conditions: 50.306 MHz, pw = 3.5 μs; ct = 5 ms; rt = 5 s; sw = 20 kHz.

^{13}C CP/MAS-NMR was carried out at 50.306 MHz, $\pi/2$ pulse width 3.5 μs, contact time 5 ms, relaxation time 5 s, and sweep width 30 kHz. Due to carbon loadings of less than 10% by weight on the catalyst, acquisitions of about 10,000 transients were required to obtain adequate *S/N* ratios. An external sample of adamantane was used to reference the spectra to TMS. The NMR apparatus used was a Bruker CXP-200. Spinning rates of greater than 5 kHz were used on all samples. Spinners were Doty

TABLE 2

Effects of Time on Stream on Total Aromatic and Aliphatic NMR Signal

	TOS = 20 s		TOS = 120 s		TOS = 900 s	
	Area	Area%	Area	Area%	Area	Area%
Aliphatic	18.10	42.11	8.71	41.39	8.75	44.09
Aromatic	22.62	52.63	11.03	52.44	9.90	49.84
Bridge	1.26	2.94	0.30	1.42	0.21	1.04
Standard	1.0000	2.33	1.0000	4.75	1.0000	5.04
Total	42.976	100.0	21.035	100.0	19.856	100.0
Arom/Nonarom		1.17		1.22		1.10

Note. Areas were normalized to give an area of 1 to the "reference peak which resulted from the spinner vial cap and is constant from run to run. "Bridge" denotes structure found at −2 ppm.

single-crystal industrial sapphire vials. The top cap was made of Kel-F, which does not produce a ^{13}C CP/MAS-NMR signal, while the bottom was of Vespel. The Vespel cap in this position emits small ^{13}C signals at 165.9 and 155.7 ppm. The peak at 165.9 was used to normalize the areas of the various peak groups found in the spectra by assigning its area a value of 1.

^{29}Si MAS-NMR was conducted at 39.740 MHz, $\pi/2$ pulse width 3.0 μs, relaxation time 10 s, and sweep width 20 kHz. Samples were referenced with TMS.

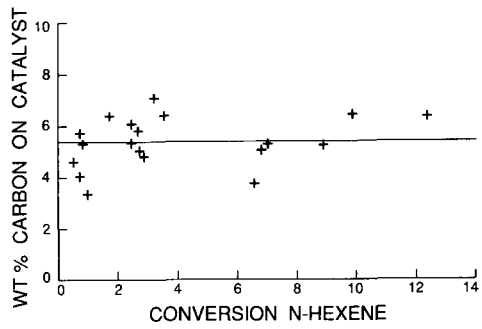

FIG. 2. Integral conversion effects on carbon on catalyst. Reaction conditions: 305°C; time on stream and catalyst-to-reactant ratio as per Table 1.

RESULTS

NMR Analysis

The use of ^{13}C CP/MAS-NMR spectroscopy gives us a detailed picture of the structural groups present in the coke. The spectra (Fig. 1) have a dominant peak at ca. 130 ppm which corresponds to sp^2 bonded carbons. Further downfield at chemical shifts of ca. 135 ppm, the resonance peaks represent alkylated aromatics and carbon bridges between aromatic rings (*6–8*). Peaks in the 140- to 150-ppm range correspond to polyalkylated aromatic species. In the aliphatic region distinct groupings of resonance peaks which correspond to primary, secondary, and tertiary carbons in various electronic environments are observed. The observation of a peak at ca. -2 ppm is quite unusual. This peak is present at all times on stream examined.

The effect of time on stream (TOS) on the ^{13}C spectrum of the coke is illustrated in Fig. 1 and quantified in Table 2. The ratio of the normalized signal intensities of aliphatic and aromatic carbon, as measured by their respective areas, remain constant with time ($\pm 10\%$). This indicates that the irreversibly adsorbed surface species reach a structural steady-state rapidly and change very little with increased TOS in the period 20 to 900 s.

On the other hand the ^{29}Si MAS-NMR spectra (Fig. 4) show a considerable broadening of the Si(1Al) and Si(0Al) peaks (-102 and -107 ppm, respectively) with TOS. The source of the line broadening in the silicon spectra is not obvious. Factors which may be involved in the broadening observed here are the structure, concentration, and distribution of the coke as well as the presence of free radical species in the coke. The original linewidths were fully restored upon regeneration of the catalyst by combustion.

Elemental Analysis of Coke

By regenerating the catalyst and trapping the H_2O and CO_2 produced, the amounts of carbon and hydrogen in the coke were determined for various experimental runs. Figure 2 shows that the weight of carbon on catalyst is relatively constant with integral conversion while as a function of TOS it increases rapidly in the first few seconds of reaction and shows little increase with further TOS as illustrated in Fig. 3. Using

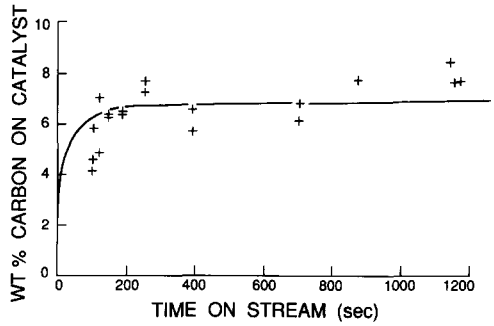

FIG. 3. Reaction time effects on carbon on catalyst. Reaction conditions: 305°C; conversion and catalyst to-reactant ratio as per Table 1.

TABLE 3

Minor Products Found in Concentrate: Acyclic Paraffins

Alkyl group	Carbon number								
	7	8	9	10	11	12	15	18	21
Normal	D	D	D	D	D	D	D		
Methyl-	D	D	D	D	D	D		D	
Dimethyl-	D	D	D	D	D	D			D
Trimethyl-			D			D			
Ethyl		D							
Ethyl methyl			D						
Ethyl Dimethyl			D						

Note. Products of oligimerization and rearrangement of the feed followed by cracking to produce a gas-phase paraffin and a dehydrogenated surface species. D denotes a product detected in the concentrate.

TABLE 5

Minor Products Found in Concentrate: Acyclic Diolefins

Alkyl group	Carbon number							
	7	8	9	12	13	15	17	18
Normal								
Methyl-	D				D			
Dimethyl-	D	D		D			D	
Trimethyl-			D			D		D
Ethyl								
Ethyl methyl			D					
Ethyl dimethyl								

Note. Desorbed products of reactions which could yield the products of Table 3. These were detected in trace amounts only. D denotes a product detected in the concentrate.

the Si/Al_{FW} of the catalyst and the unit cell formula of a Y zeolite, the ratio of carbon atoms in the coke to aluminum atoms in the catalyst framework (C/FAl), as conversion approaches zero, was determined to be 4.2 (see Appendix for detailed calculation).

GC-MS Analysis

Tables 3 to 8 present a listing of minor products of *n*-hexene cracking on USHY observed in our studies and those reported earlier by Abbot and Wojciechowski (*9*). Reaction temperature was found to affect only the relative concentration of the products and not the species present, indicating that the same reactions occur over the 200°C range examined. In concentrated samples obtained from the runs at 305°C with less than 2% integral conversion, significantly more saturated species and larger oligomers were detected than those in concentrates from higher integral conversion and higher temperature experiments.

From Tables 6 to 8 it is seen that all the cyclic products detected are alkylated; methyl groups are the most common side chain present while butyl side chains are the longest and least frequently observed. It is also seen that cyclohexenyl rings are rare and that most six carbon rings are aromatic.

TABLE 4

Minor Products Found in Concentrate: Acyclic Mono Olefins

Alkyl group	Carbon number														
	7	8	9	10	11	12	13	14	15	16	17	18	19	20	21
Normal	D	D	D	D	D	D		D							
Methyl-	D	D	D	D	D	D	D	D							
Dimethyl-	D	D	D	D	D	D					D			D	
Trimethyl-			D			D		D				D			D
Ethyl		D	D	D		D									
Ethyl methyl						D									
Ethyl dimethyl															

Note. Products of oligimerization and rearrangement of the feed followed by β-scission to form olefinic products in the gas phase and on the surface. D denotes a product detected in the concentrate.

TABLE 6

Minor Products Found in Concentrate: Cyclics

	5(p)	6(p)	5(o)	6(o)
Methyl-	D/P	D	D/P	
Dimethyl-	D/P	D/P	D/P	P
Trimethyl	D/P	D/P	D/P	P
Ethyl methyl	D/P		D/P	P
Ethyl propyl		D/P		D/P
Ethyl dimethyl	P		D/P	P
Dipropyl				D

Note. The cyclic olefins are the major product associated with the formation of the products in Table 3. Cyclic paraffins are associated with the olefins shown in Table 4. Ring size: 5(o) denotes C5 olefinic ring; 6(p) denotes C6 paraffinic ring. P denotes a product predicted by the proposed cyclization reaction. D denotes a product detected by GC-MS analysis.

TABLE 7

Minor Products Found in Concentrate: Aromatics

	B	N	A	P
Methyl-	D			
Dimethyl-	D	D		
Trimethyl	D	D	D	D
Tetramethyl	D		D	D
Hexamethyl	D			
Ethyl	D			
Diethyl	D			
Triethyl	D			
Propyl	D			
Isopropyl	D			
Dipropyl	D			
Methyl ethyl	D			
Methyl propyl	D			
Methyl pentyl	D			
Me triethyl	D			
DM ethyl	D			
DM propyl	D			
DM butyl	D			
DM isobutyl	D			
DM diethyl	D			
Dipropyl	D			
Triethyl	D			

Note. Species are formed by cyclization of oligomers followed by successive dehydrogenation reactions. B, benzene; N, naphthalene; A, anthracene; P, phenanthrene. D denotes a product detected in the concentrate.

TABLE 8

Minor Products Found in Concentrate: Alkylated Polycyclics with the Cyclic Structure Shown Below

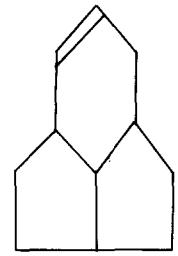

Note. Species with this basic framework were detected up to and including C_{21} species. They are believed to be intermediates in the formation of polycyclic aromatics.

Five-membered carbon rings are the smallest cyclic structures detected and, significantly, five-membered cycloolefins are an important minor product.

Alkylated polynuclear aromatic species with up to three fused rings were found in the liquid products. Methyl groups were the only alkyl group observed on these species. Olefinic polycyclic species with three fused rings were also detected in the C_{12} to C_{21} range. The largest aromatic structures detected were tetramethylanthracene and tetramethylphenanthrene, both C_{18} molecules.

The concentrated products also contained trace amounts of acyclic diolefins and various paraffins and olefins up to and including C_{21} species (Tables 3 to 5). The presence of C_{21} species at conversions of about 1% indicates that feed tetramers are likely formed. We also note that the formation of acyclic paraffinic species from the oligomer generally proceeds by the fragmentation of the oligomer in groups of three. Thus C_{21}, C_{18}, and C_{15} paraffins are all detected but not species with intermediate chain lengths. This distinctiion is not as apparent with the acyclic olefinic oligomers.

DISCUSSION

NMR Results

Previous ^{13}C CP/MAS-NMR studies of

coke by Weitkamp and Maixner (*10*), Neuber *et al.* (*11*), Maixner *et al.* (*12*), and Fleisch *et al.* (*13*) have produced spectra similar to ours with the exception of the peaks near −2 ppm observed in this study. Such similarity in the spectra is quite remarkable, considering the different reaction conditions and feedstocks used in these studies. The earlier studies show that even at very long reaction times significant amounts of aliphatic structures are present in the coke. Fleisch *et al.* (*13*) have also shown that at high reaction temperatures the amount of aliphatic structure in the coke is much less than that observed under less severe conditions.

Our ^{13}C-CP/MAS-NMR spectra show that even at very short times on stream the coke has a significant sp^2 character and that alkylated and polyalkylated aromatic species are common. The only peaks which were unexpected are those near −2 ppm. Methyl groups are evident at ca. 13 ppm and were expected to be the furthest upfield peak. Considering the reaction conditions under which these coke structures were formed, it is doubtful that the −2 ppm peak is due to cyclopropyl groups. The other possible source of this peak is shielding interactions between aromatic ring structures and "neighboring" aliphatic structures. From basic NMR theory (*14*) a carbon atom which lies directly over an aromatic ring will experience considerable shielding from the induced magnetic field. This will cause its observed chemical shift to move upfield. It is this phenomenon which we believe is responsible for the peak observed at −2 ppm. This suggests that some of the coke may be formed in close, overlapping layers since it is unlikely that the source of the highly shielded peak could be attached to the shielding source.

Figure 1 also shows that the ^{13}C spectrum of the coke changes very little with time on stream (TOS) between 20 and 900 s. By assigning the peak at 165.9 ppm an area of 1, the relative areas under the aromatic peaks from ca. 120 to 150 ppm can be compared with the areas under the aliphatic portion of the spectra. The results of such an analysis (Table 2) confirm the visual observations of Fig. 1: the structure of the irreversibly adsorbed species does not change significantly over the reaction times studied.

Using the kinetic model presented by Abbot and Wojciechowski (*15*) the half life of the catalyst for this system at 305°C was determined to be 1 s. That the coke shows no appreciable change in its structure over the times on stream examined here is a qualitative confirmation of the kinetic model; the catalyst is essentially completely deactivated by 20 s. Further changes in the structure of the irreversibly adsorbed surface species must be due exclusively to noncatalyzed reactions, e.g., thermal or free radical reactions. The unchanging ^{13}C CP/MAS-NMR spectrum with time on stream indicates that these reactions are slow to induce detectable structural changes in the coke when compared with the initial catalytic reactions.

The ^{29}Si MAS-NMR spectra (Fig. 4) indicate that there are significant electronic interactions between the framework silicon atoms and the coke. This appears to contradict the CEEL spectroscopy results of Fleisch *et al.* (*13*), which indicated no interaction at all. Because of the "poisonous" nature of coke to catalytic reactions, we find it difficult to imagine that the presence of this material does not influence the electron distribution around the silicon atoms in some fashion. The quantity and structure of an adsorbant has been found to affect the ^{29}Si MAS-NMR spectra of zeolites (*16–18*). It is found here, however, that considerable broadening occurs after 20 s time on stream, when structural changes in the coke have apparently ceased and the coke loading per gram of catalyst is constant (Fig. 3). Thus, these two factors are not contributors to the broadening after 20 s TOS.

The presence of free radicals in the coke could, by decreasing the T1 (spin-lattice relation time constant) of neighboring silicon atoms, be a source of line broadening. When

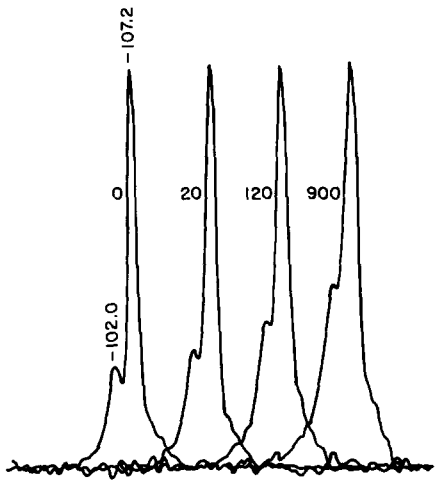

FIG. 4. Reaction time effects on ^{29}Si MAS-NMR spectra. Reaction conditions as per Fig. 1. NMR experimental parameters: 39.740 MHz; pw = 3.0 μs; rt = 10 s; sw = 20 kHz. Spectra are unenhanced.

the ^{29}Si MAS-NMR experiment was repeated with a shorter delay (relaxation time = 1 s), it was observed that the linewidth remained unchanged, suggesting that free radicals are not a significant factor here.

Another possible source of the broadening is the distribution of the coke molecules in the zeolite crystals. Broadening from this source could occur if, while the coke was being formed, it remained localized, e.g., at the active sites. If the coke redistributes after deactivating the catalyst, the number of electronic environments of the silicon atoms will increase initially, causing a broadening of the observed silicon linewidth. As the coke distribution continues and becomes more homogeneous over the catalyst, the number of possible electronic environments of the silicon atoms should pass through a maximum, then decrease, until, at a uniform coke distribution no further change in the silicon linewidth occurs.

To investigate whether such a process was occurring, the unenhanced silicon spectra were deconvoluted assuming a Lorentzian lineshape. The individual linewidths of the Si(1Al) and Si(0Al) peaks are shown in Fig. 5 as a function of TOS. Although the data are limited, the Si(1Al) peak appears to follow the pattern described above, suggesting that it is the distribution of the coke on the catalyst crystallites which is the dominate factor in the line broadening observed. It is not evident from our limited data whether the same pattern is repeated with the Si(0Al) peak. That the patterns of the Si(1Al) and Si(0Al) peak widths differ from one another suggests that the Si(1Al) sites are not homogeneously distributed in the zeolite crystal.

Elemental Analysis

Elemental analysis of the coke allows the determination of the ratio of carbon atoms in the coke (C) to aluminum atoms in the catalyst framework (FAl). For the initial coke loading of 6.4% carbon on catalyst (Fig. 2), obtained for experimental runs at 305°C, the ratio of C/FAl is 4.2 while the bulk C/Al ratio is 1.3. From the stoichiometry of coke formation (*1*), the initial coke was found to have an average chain length of 5.1. Therefore a maximum of 84% of the FA1 (4.2 carbon atoms per FAl divided by five carbon atoms per initial coke molecule) are initially active in coke formation. The percentage of initially active FA1 for reactant conversion must be greater than or equal to that for initial coke formation. From

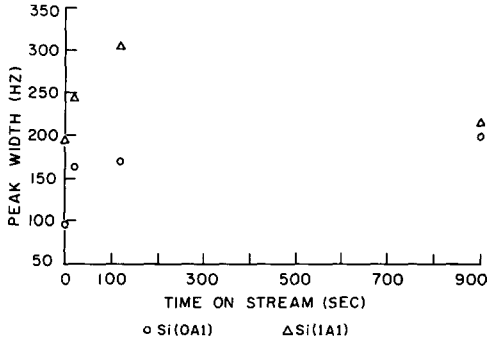

FIG. 5. Deconvoluted ^{29}Si linewidths. Linewidths were obtained by deconvolution of the unenhanced ^{29}Si spectra of Fig. 4, assuming a Lorenztian lineshape.

the ^{29}Si NMR linewidths discussed earlier, it would appear that the actual fraction of FAl involved in forming coke from all sources is much smaller than the above-predicted upper bound.

Magnoux *et al.* (*3*) have conducted chemical extraction experiments on a coke they produced from the reaction of propene on a USHY catalyst at 300°C. Using their figures for a reaction time of 1800 s (30 min) (Table 2 of Ref. (*3*)) the ratio of carbon atoms to bulk aluminum can be determined using the H/C ratio, coke loading, and catalyst information given. This value is calculated to be 1.3 carbon atoms per bulk Al, which is the same as our bulk value. Unfortunately, we do not know the amount of framework aluminum in their catalyst; however, by using the number of Al atoms for which the NH_3 heat of adsorption was greater than 100 KJ/mol, a comparable figure should be obtained. The number of carbon atoms per such an aluminum atom is 9.8. In our experiments the carbon loading at 1200 s (20 min) time on stream (Fig. 3) gives a C/FAl of 5.2. Given the different feedstocks used and somewhat different basis for obtaining these figures these results are remarkably similar. The dangers in using these figures to correlate coke to catalyst activity becomes evident. Elemental analysis in our work and that of Magnoux *et al.* suggests that complete deactivation occurs at coke loadings of about five carbon atoms per framework aluminum atom. The silicon NMR results present a much different picture. It suggests deactivation occurs while the coke is highly localized and electronically influencing only a fraction of the potential active sites.

Our ^{13}C CP/MAS-NMR spectra show that the transition of the irreversibly adsorbed species from their initial structure to their steady-state structure is very rapid and occurs in the same time frame as the decline in catalytic activity. This suggests that the loss in activity may be related to events occurring in the pathological reactions which lead to the aromatic species detected by Magnoux *et al.* (*3*), by us, and by others. If this is the case then it would seem that it is the early pathological reactions which lead to deactivation while, after the catalyst is deactivated, subsequent rearrangements merely seek to reduce the energy of the surface layer on the catalyst. To take a typical coke species detected after dissolution of a catalyst coked for 30 min time on stream and to relate it to the deactivation process which in all probability occurred in the first few seconds of reaction will not lead to a meaningful picture of the process of deactivation.

Mechanisms in Minor Product Formation

(*i*) *Oligomerization.* With the exception of methylcyclopentene (MCP) all cyclic products detected using GC-MS analysis are C_7 or larger and therefore are associated with the oligomerization process which occurs with olefins on acid catalysts. We therefore begin with a description of this process.

Oligomerization and disproportionation have been proposed by several authors as the route of olefin conversion on solid acid catalysts. In support of this, isotopic studies (*21, 22*) have shown that a carbenium ion can act as a "Lewis acid" to a gas-phase olefin by accepting an electron from the double bond, thus forming a bond to the approaching gas-phase species. Such a reaction results in the formation of a surface dimer. These studies have also indicated that such reactions between surface species and olefinic gas-phase molecules are common at temperatures of interest to catalytic cracking. In addition they have shown that the hydrogen atoms of surface species are frequently interchanged with those of the gas-phase species without the formation of an oligomer. A notable exception to this hydrogen "scrambling" are hydrogen atoms in primary positions. These observations fit well with the known reactivity of hydrogen atoms in hydrocarbons, viz., tertiary > secondary > primary.

The most likely position for the oligomer-

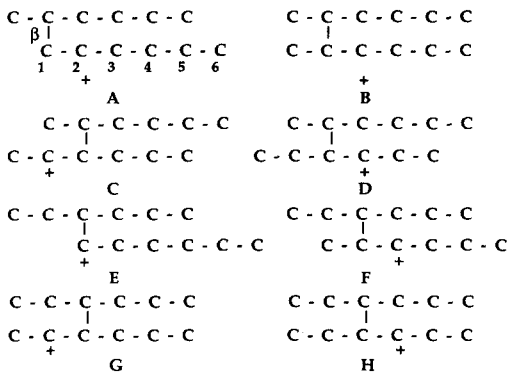

FIG. 6. Possible dimers of *n*-hexene. Dimers formed from combinations of 1-, 2-, and 3-hexene.

ization reaction to occur is at the cationic center of the surface carbenium ion. Using this assumption, the possible dimer species from *n*-hexyl carbenium ion and *n*-hexene are shown in Figure 6. The C_{12} olefins corresponding to these surface species—methyl undecenes, dimethyl decenes, ethyl decenes, ethyl methyl nonenes, and diethyl octenes—have been found by GC-MS analysis of the concentrated products. These dimers will be used as the starting point of a proposed cyclization reaction, although we do not mean to imply that other dimers cannot be formed at higher conversions.

(ii) Cyclization. It has been generally assumed in the literature that cyclization occurs via the Diels–Alder cycloaddition reaction. For such a reaction to occur with carbocations as intermediates, the presence of acyclic diolefins and triolefinic precursors is necessary. Diolefins were found to be present only in trace quantities in the concentrates, while no triolefinic products were detected. In addition, methylcyclopentene was observed to be a primary product of the reaction (having no detectable gas-phase intermediates to its formation) (*1*). Examination of the other primary products leads to the conclusion that the formation of this product from a dimer of the feed necessitates (by stoichiometry) the formation of a C_6 paraffin. This observation suggests that the Diels–Alder cycloaddition reaction is not the mechanism by which methylcyclopentene is formed and that another mechanism for cyclization must be sought.

It is well established that the C–C bond at the β position is the weakest bond in a carbenium ion. This is therefore a likely position for a cyclization reaction to take place. Starting with the initial C_{12} dimer carbocation "A" or "E" (Fig. 6), we postulate that a cyclopentyl ring is formed by rupture of the β bond and attachment of carbon 1 to 5 as shown in Fig. 7. One of the secondary hydrogen atoms attached to carbon 5 is simultaneously displaced to the leaving species, in this case *n*-hexane. The resulting surface species is the methylcyclopentyl carbocation which upon desorption gives methylcyclopentene. Such a displacement mechanism is a slight modification to the "normal" β-scission reaction, differing only in that the leaving group accepts a hydrogen atom from a distant carbon, forcing cyclization to take place. By comparing the initial selectivities of methylcyclopentene and *n*-hexene (*1*), we find that this hydrogen displacement reaction accounts for about 13% of the initial *n*-hexane formed. The remaining 87% results from other hydrogen transfer reactions.

Using this hydrogen displacement mechanism and the dimers shown in Fig. 6, the formation of various cyclic species can be predicted. Two constraints were imposed upon the cyclization mechanism. The first is that primary hydrogen is not involved in the cyclization reaction, and the second is that the cationic center of the dimer can shift only by two carbon atoms before the displacement reaction will occur. The first restriction is applied because hydrogens in primary positions are known to be unreactive. The second stems from an examination of the primary products of skeletal isomerization. Two hydride shifts will account for all skeletal isomers observed (*1*).

The mechanism predicts nearly all of the nonaromatic cyclic species detected (Table 6), while the products which are predicted but are not observed are cyclic carbocations

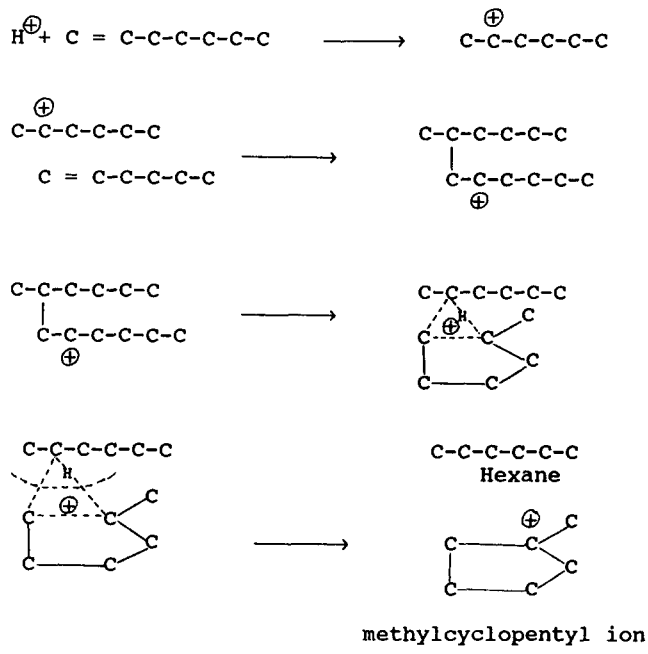

FIG. 7. Proposed cyclization mechanism. Cyclization of reactant dimer via hydrogen displacement reaction.

which we believe have undergone further reactions such as dealkylation, alkylation, rearrangement, and aromatization. We also point out that by excluding primary hydrogens from taking part in hydrogen displacement reactions, all cyclic species predicted will be alkylated. This makes the mechanism conform to the observed absence of nonalkylated cyclic species.

(*iii*) *Dehydrogenation of surface species.* Once cyclization of the surface species has occurred, dehydrogenation to an aromatic appears to be a very rapid process. This is especially true for six-membered rings, since partially dehydrogenated molecules such as cyclohexenes are rare and cyclodiolefins were not observed. The presence of small amounts of acyclic dienes indicated that dehydrogenation reactions can also occur on acyclic carbenium ions but to a much smaller extent than in cyclic species. This is not surprising since linear carbenium ions can more easily undergo β-scission and desorption while five and six carbon cyclic carbenium ions are quite resistant to cracking (*23*).

The exact mechanism by which dehydrogenation occurs is unclear. One plausible mechanism is that monomolecular elimination of small chain paraffins and molecular hydrogen occurs, leaving a dehydrogenated surface species. This process allows for the required electroneutrality of the catalyst surface and could explain the presence of products which are normally the result of pyrolytic reactions. Such species are secondary products of *n*-hexene cracking on USHY (*1*) and have been shown to be secondary products in most catalytic cracking studies, irrespective of reactant type. The generalized pathway from *n*-hexene to aromatic product is presented in Fig. 8.

(*iv*) *Catalyst deactivation.* The species which are detected as coke are likely a distorted reflection of the species which cause decay under reaction conditions. If a surface species becomes highly dehydrogenated, the probability that it will desorb from the

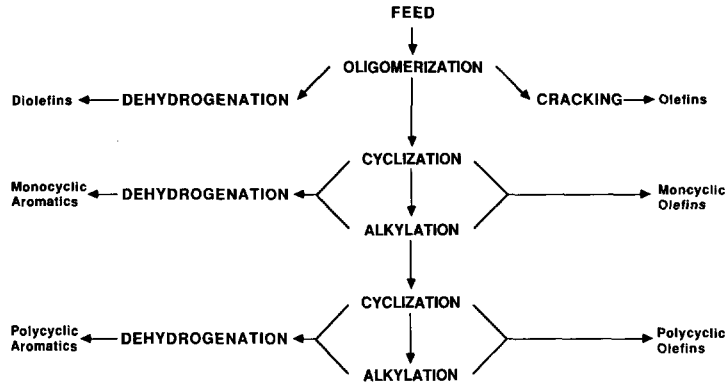

FIG. 8. Reaction pathways in the formation of minor products. The spectrum of minor products observed suggests this generalized pathway for their formation from *n*-hexene. A definite progression of dehydrogenated species toward aromatic product was noted.

catalyst surface is reduced and it will likely be detected as "coke" at the end of a run. However, the observation that a particular species has not undergone desorption before the reaction is stopped or during the postreaction purging does not imply that it is responsible for deactivation. Rather, some of these surface species still have the potential to be involved in hydrogen transfer or other reactions and thus contribute to the conversion of the feed. On the other hand some strongly inhibiting or deactivating species may be stripped during the postreaction purging and not be measured as coke. Our minor products contain both mono- and polynuclear aromatic species which may well fall into the latter category.

From the chemistry described above, it seems that the structure and reactivity of the species present on the surface during the cracking reaction are dynamic, changing with time and conversion. Our kinetic model indicates that the half life of the catalyst at 305°C is 1 s, while the elemental analysis of the coke indicates that the catalyst is completely deactivated at C/FAl ratios of between 4 and 5. At the same time the irreversibly adsorbed surface species were found to attain a structural quasi-steady state in the first 20 s of reaction time, as observed in the ^{13}C CP/MAS-NMR spectra. Furthermore, the ^{29}Si MAS-NMR spectra indicate that the distribution of these irreversibly adsorbed species, after cracking reactions have ceased, progresses from one in which only a few potential active sites are affected by the coke during the first 20 s of reaction to a more homogeneous distribution as time on stream increases.

The combination of reaction chemistry, NMR, elemental analysis, and kinetic modelling provides an interdependent and interesting picture of the deactivation process in this system. Deactivation does not appear to be tied to any one event. The chemistry suggests that as the reaction surface builds with products of increasing aromaticity, the activity of the catalyst decreases. The elemental analysis of the coke and evidence of its redistribution after cracking ceases imply that only a fraction of the framework aluminum atoms are ever active in this system. The ^{29}Si NMR results, which point to the slow redistribution of the coke on a deactivated catalyst, suggest that the active sites for *n*-hexene conversion at 305°C may be only those framework aluminums found on or near the surface of the zeolite crystallites.

CONCLUSIONS

By combining the chemistry and kinetics of this system with multinuclear MAS-NMR spectroscopy and elemental analysis of the coke, a unique picture has emerged of how

this material may be related to the deactivation phenomenon. The reaction chemistry indicates that, as the surface species become more dehydrogenated, reactions which convert *n*-hexene to products are inhibited, suggesting that the deactivation phenomenon is not a single event but rather a series of reaction events which result in a surface of decreasing reactivity. ^{13}C CP/MAS-NMR spectra show that the surface species which are detected as coke attain a structural steady state in the same time frame as that for complete catalyst deactivation, supporting the "deactivation by inhibition" proposal.

^{29}Si NMR analysis suggests that coke is initially formed in highly localized regions and that, when compared to the time frame of the deactivation process, it migrates slowly over the catalyst surface to become more homogeneously distributed with increased time on stream. This evidence, combined with the 1-s half life of the catalyst and a deactivated catalyst coke loading of four to five carbon atoms per framework aluminum, suggests that reactant conversion and coke formation in this system occur on or near the exterior surfaces of the zeolite crystallite.

APPENDIX: CALCULATION OF CARBON-TO-ALUMINUM RATIO

The general formula of NaHY type Faujausite is

$$Na_xH_{(56+y-x)}(AlO_2)_{56+y}(SiO_2)_{136-y}.$$

The framework Si/Al ratio is given by

$$(Si/Al)_{FW} = (136 - y)/(56 + y)$$

and

$$(Si)_{FW} = 192 - (Al)_{Fw}; \; (Al)_{FW} = 192 - (Si)_{FW},$$

where $(Si)_{FW}$ and $(Al)_{Fw}$ represent the number of Si and Al atoms in the framework per unit cell.

In addition it can be easily shown that

$$(Al)_{FW} = 192/[1 + (Si/Al)_{FW}],$$

based upon the assumption that upon dealumination during the exchange/calcination process the vacancy left by the aluminum is filled by a silicon atom.

Therefore, the unit cell weight of a fully exchanged USHY catalyst is

$$UC_{wt} = 11{,}536 - 0.0965(Al)_{FW} \text{ [grams/uc]}$$

and the atomic ratio of carbon in the coke to framework aluminum will be given by

$$\left\{\frac{C}{Al}\right\}_{FW} = \frac{(\text{wt Carbon})/12}{(\text{wt Cat})} \times \left\{\frac{11{,}536 - 18.528/[1 + (Si/Al)_{FW}]}{192/[1 + (Si/Al)_{FW}]}\right\},$$

where the weights of carbon and catalyst are in grams.

ACKNOWLEDGMENTS

We acknowledge with thanks the assistance of Ms. S. Blake with the NMR spectroscopy and the financial assistance of Imperial Oil, Ltd., and the National Science and Engineering Research Council of Canada.

REFERENCES

1. Groten, W. A., and Wojciechowski, B. W., *J. Catal.*, **122,** 362 (1990).
2. Gallezot, P., Leclercq, C., Guisnet, M., and Magnoux, P., *J. Catal.* **114,** 100 (1988).
3. Magnoux, P., Roger, P., Fouche, V., Gnep, N. S., and Guisnet, M., *in* "Studies in Surface Science and Catalysis" (B. Delmon and G. F. Fromont, Ed.), p. 317. Elsevier Science, Amsterdam, 1987.
4. Engelhart, G., and Lohse, U. *Zeolites* **2,** 59 (1982).
5. Ko, A. N., and Wojciechowski, B. W., *Prog. React. Kinet.* **12**(4), 201 (1984).
6. Marshall, J. L., "Carbon–Carbon and Carbon–Proton NMR Couplings," *in* "Methods in Stereochemical Analysis," Vol. 2. Verlag Chemie Inter., Deerfield Beach, 1983.
7. Sudmeijer, O., Wilson, A. E., and Hays, G. R., *Org. Magn. Reson.* **22**(7), 459 (1984).
8. Veeman, W. S., *Prog. NMR Spectrosc.* **16,** 193 (1984).
9. Abbot, J. A., and Wojciechowski, B. W., *Canad. J. Chem. Eng.* **63,** 278 (1985).
10. Weitkamp, J., and Maixner, S., *Zeolites* **7**(1), 6 (1987).
11. Neuber, M., Ernst, S., Geerts, H., Grobet, P. J., and Jacobs, P. A., "Catalyst Deactivation" *in* "Proceedings, 4th Inter. Sympos.," p. 567. Elsevier, Amsterdam, 1987 [*Stud. Surf. Sci. Catal.*, Vol. 34].

12. Maixner, S., Chen, C. Y., Grobet, P. J., Jacobs, P. A., and Weitkamp, J. *in* "7th Inter. Zeolite Conf." (Y. Murakami, A. Iijima, and J. W. Ward, Eds.), p. 693. Kodansha, Tokyo and Elsevier, Amsterdam, 1986.
13. Fleisch, T. H., Zajac, G. W., Meyers, B. L., Ray, G. J., and Miller, J. T., *in* "Proceedings, 9th International Congress on Catalysis, Calgary, 1988" (M. J. Phillips and M. Ternan, Ed.), Vol. 1, p. 483. Chem. Institute of Canada, Ottawa, 1988.
14. Pople, J. A., Scheider, W. G., and Berstein, H. J., "High Resolution Nuclear Magnetic Resonance Spectroscopy," p. 181. McGraw–Hill, New York, 1959.
15. Abbot, J. A., and Wojciechowski, B. W., *Canad. J. Chem. Eng.* **66,** 817 (1988).
16. West, G. W., *Aust. J. Chem.* **37,** 455 (1984).
17. Fyfe, C. A., O'Brien, J. H., and Strobl, H., *Nature (London)* **326,** 281 (1987).
18. Fyfe, C. A., Strobl, H., Kokotailo, G. T., Kennedy, G. J., and Barlow, G. E., *J. Amer. Chem. Soc.* **110,** 3373 (1988).
19. Lange, J. P., Gutsze, A., and Karge, H. G., *J. Catal.* **114**(1), 136 (1988).
20. Singer, L. S., *in* "Proceedings, 5th Conf. on Carbon," Vol. 2, p. 37. Pergamon Press, New York, 1963.
21. Gerberich, H. R., Larson, J. G., and Hall, W. K., *J. Catal.* **4,** 523 (1965).
22. Ozaki, A., and Kimura, K., *J. Catal.* **3,** 395 (1964).
23. Abbot, J. A., and Wojciechowski, B. W., *J. Catal.* **107,** 571 (1987).